A Pseudomonas sp. strain uniquely degrades PAHs and heterocyclic derivatives via lateral dioxygenation pathways

A *Pseudomonas* sp. strain uniquely degrades PAHs and heterocyclic derivatives via lateral dioxygenation pathways

Yunli Liu[a†], Haiyang Hu[a†], Giulio Zanaroli[b], Ping Xu[a] and Hongzhi Tang[a]*

[a]State Key Laboratory of Microbial Metabolism, and School of Life Sciences; Biotechnology, Shanghai Jiao Tong University, Shanghai 200240, People's Republic of China

[b]Department of Civil, Chemical, Environmental and Materials Engineering (DICAM), University of Bologna, Bologna 40131, Italy

†These authors contributed equally to this study. *Corresponding author: H. Z. Tang. Mailing address: School of Life Sciences; Biotechnology, Shanghai Jiao Tong University, Shanghai 200240, P. R. China. E-mail: tanghongzhi@sjtu.edu.cn; Tel: +86-21-34204066; Fax: +86-21-34206723.

Abstract

Polycyclic aromatic hydrocarbons (PAHs) and heterocyclic derivatives are organic pollutants that pose a serious health risk to human beings. In this study, a newly isolated *Pseudomonas brassicacearum* strain MPDS could effectively degrade PAHs and heterocyclic derivatives, including naphthalene, fluorene, dibenzofuran (DBF) and dibenzothiophene (DBT). Notably, strain MPDS is able to degrade fluorene, DBF and DBT uniquely via a lateral dioxygenation pathway, while most reported strains degrade fluorene, DBF and DBT via an angular dioxygenation pathway or co-metabolize them via a lateral dioxygenation pathway. Strain MPDS completely degraded 50 mg naphthalene (in 50 mL medium) in 84 h, and OD_{600} reached 1.0−1.1; while, it stabilized at OD_{600} 0.5–0.6 with 5 mg fluorene or DBF or DBT. Meanwhile, 65.7% DBF and 32.1% DBT were degraded in 96 h, and 40.3% fluorene was degraded in 72 h, respectively. Through genomic and transcriptomic analyses, and comparative genomic analysis with another DBF degradation strain, relevant gene clusters were predicted, and a naphthalene-degrading gene cluster was identified. This study provides understanding of degradation of PAHs and their heterocyclic derivatives, as well as new insights into the lateral dioxygenation pathway of relevant contaminants.

Keywords: PAHs Degradation; Heterocyclic Derivative; *Pseudomonas*; Lateral Dioxygenation Pathway

1. Introduction

Polycyclic aromatic hydrocarbons (PAHs) are organic pollutants that are composed of two or more benzene rings (Haritash & Kaushik, 2009), such as naphthalene and fluorene. Heterocyclic aromatic hydrocarbons are compounds with other elements composing the ring structures like dibenzofuran (DBF) and dibenzothiophene (DBT). The main anthropogenic sources of PAHs and heterocyclic derivatives are from incomplete combustion of fossil and solid biomass fuels, high-temperature industrial processes and petroleum refinery effluents (Sakshi et al., 2019). About 116,000 tons of PAHs have been produced since 2003 (Xu et al., 2006; Zhang et al., 2008), causing environmental pollution and threatening human health. Fluorene is a tricyclic aromatic hydrocarbon with a strong toxic effect, and its heterocyclic derivatives (DBF and DBT) pose a serious health risk to human beings, resulting in deformities, cancer, gene mutation and chromosome aberration through breathing or direct skin contact (Sakshi & Haritash, 2020).

Considering physical and chemical treatments of PAHs are energy, cost, chemical intensive, and even causing secondary pollutants, bioremediation is ecofriendly and sustainable, and has recently gained considerable attention in the last two decades (Sakshi et al., 2019). Several microorganisms that could utilize fluorene, DBF or DBT were screened and discovered, including *Pseudomonas* (Fortnagel et al., 1990; Grifoll et al., 1995; Li et al., 2009), *Sphingomonas* (Wilkes et al., 1996; Gai et al., 2007), *Rhodococcus* (Aly et al., 2008), *Burkholderia* (Gregorio et al., 2004), *Rhizobium meliloti* (Frassinetti et al., 1998), and *Terrabacter* (Schmid et al., 1997; Kasuga et al., 2013). However, these reported strains only

utilize one of those pollutants as the sole carbon, or degrade DBF or DBT by co-metabolism with other compounds. For example, Becher (2000) and Li (2009) respectively found *Ralstonia* sp. strain SBUG 290 and *P. putida* B6-2, which could co-metabolize DBF in cultivation with biphenyl. *Arthrobacter* sp. P1-1 capable of co-metabolizing DBT with phenanthrene was identified (Seo et al., 2006). These strains lack the ability to utilize DBF or DBT independently, and few strains could degrade these three substrates simultaneously.

Through technologies of genomics, proteomics, transcriptomics and metabolomics, researchers analyzed the microbial degradation pathways and genetic information of PAHs (Sakshi & Haritash, 2020). Diverse clusters of PAH-catabolic genes such as *nah, pah, nid, dox, phn, phd, nag, fln* were discovered in past research studies and the degradation pathways of PAHs have been given more attention (Sakshi & Haritash, 2020). In recent years, various degradation pathways of fluorene, DBF and DBT have been studied. There are two kinds of biodegradation pathways for these three compounds: an angular dioxygenation pathway and a lateral dioxygenation pathway. As for angular dioxygenation pathway, fluorene is transformed into 9-fluorenol, 9-fluorenone and 1,9a-dihydroxy-1-hydrofluoren-9-one step by step (Trenz et al., 1994; Nojiri et al., 2002; Nojiri et al., 2001; Wattiau, et al., 2001). Then, after several uncertain steps, it is further catabolized to phthalic acid, which can be fully biodegraded by many microorganisms. Luc Schuler found that genes *flnA* and *flnB* are responsible for the angular oxidation of fluorene, 9-fluorenol and 9-fluorenone (Schuler et al., 2008). Another degradation pathway of *Arthrobacter* sp. F101 proposed by Casellas et al. (1997) starts with the

lateral dioxygenation at C-3,4. After two-step oxidations and oxidative decarboxylation, it could be transformed into 2-hydroxycinnamic acid. However, the related genes in this pathway have rarely been reported. Lateral dioxygenation degradation pathways of DBF and DBT are quite similar to that of fluorene. Li (2009) reported that the biphenyl gene cluster of *P. putida* strain B6-2 generated HOBB (3'-Oxo-3'H-benzofuran-2'-yliden)but-2-enoic acid) by DBF lateral dioxygenation degradation pathway; DBT could be catalyzed into 1,2-dihydroxy-dibenzothiophene, 4-[2-(3hydroxy)-thianaphthenyl]-2-oxo-3-butenoic acid and 3-hydroxy-2-formyl-phenylthiophene. However, the genes and functional enzymes related to this degradation pathway were rarely reported.

In addition to the lateral dioxygenation degradation pathway, DBF and DBT could also be degraded in the angular dioxygenation pathway, with the attack of C-4 and C-4a at the first step. Compared with the lateral dioxygenation degradation pathway, related genes in the angular dioxygenation pathway were widely studied in recent years (Ji et al., 2017; Shi et al., 2013). Genes *dbfA* and *dfdA* encode dibenzofuran 4,4a dioxygenase that transforms DBF into cis-4,4a-dihydroxy-4,4a dihydrodibenzofuran (Sukda et al., 2009). Genes *dbfb* and *dbfc* covert cis-4,4a-dihydroxy-4,4a dihydrodibenzofuran into salicylic acid. Moreover, genes *dszABCD* are significant in DBT angular dioxygenation degradation (Ji et al., 2017; Gregorio et al., 2004; Oldfield et al., 1997), which are involved in the transformation from DBT to dibenzothiophene sulfoxide 2',3'-dihydroxybiphenyl-2-sulfinate, anthranilic acid and 2-hydroxypenta-2,4-dienoic acid. Although several key genes and enzymes of DBF and DBT degradation have been reported,

current knowledge about the fluorene, DBF and DBT complete catabolic pathways and related degradation genes are still lacking.

In this study, we isolated *P. brassicacearum* MPDS, a high-efficiency degrading strain that can utilize naphthalene, fluorene, DBF or DBT as the only carbon source. We inferred that strain MPDS degraded fluorene, DBF and DBT by lateral dioxygenation pathways on the basis of LC-MS results, which are unique compared with previous reports. We analyzed the genome and transcriptome of strain MPDS and found a naphthalene-degrading gene cluster named as *nahAFBCED*. Comparative genomic analysis with strain MPDS and another DBF degrader (*P.* strain FA-HZ1) revealed potential DBF degradation genes (Ali et al., 2019). In summary, our findings provide a further understanding of molecular mechanisms during the biodegradation of naphthalene, fluorene, DBF and DBT, and will benefit bioremediation of contaminated environments.

2. Experimental procedures

2.1. Chemicals and culture media

Naphthalene (≥ 99%, purity), dibenzofuran (DBF) and dibenzothiophene (DBT) (≥ 99%, purity) were purchased from J&K Scientific Technology Co., Ltd. Fluorene (≥ 99%, purity) was purchased from Aladdin Bio-Chem Technology Co., Ltd. Cells were cultured with LB medium and MSM medium (Lu et al., 2019). MH medium was used to detect antibiotic resistance. Preparation method of MH medium (/L): starch 1.5 g, acid hydrolyzed casein 17.5 g and beef

paste 2.0 g.

2.2. Strain isolation and identification

Pseudomonas sp. strain MPDS was isolated from the soil and mud contaminated by PAHs and petrochemicals in Tianjin (China). The soil sample was added into 50 mL MSM medium containing 0.1% yeast extract and 20 mg naphthalene. After cultivating for 7 days, a total of 1 mL mixture was added into a new flask with fresh MSM medium containing 20 mg naphthalene and cultured for 7 days. After three enrichments, a single colony was isolated on MSM plate without yeast extract. The examination of the substrates revealed that strain MPDS could utilize fluorene, DBF and DBT for growth.

The DNA of strain MPDS was extracted and primer 27F (5′-AGAGTTTGATCCTGGCTCA-3′) and 1492R (5′-CGGTTACCTTGTTACGACTT-3′) were used to sequence the whole region of 16S rRNA. The 16S rRNA sequence was alignment on BLAST (https://blast.ncbi.nlm.nih.gov/Blast.cgi). The software MEGA 5.2.2 was used to build a phylogenetic tree of strain MPDS and strains with high 16S rRNA homologous by neighbor-joining (NJ).

2.3. Antibiotic resistance detection of strain MPDS

Pseudomonas sp. MPDS grew to the exponential phase in 5 mL sterilized LB medium and measured OD_{600} with UV spectrophotometer. The OD_{600} of bacterial solution was regulated as

the same as 0.5 M standard turbid solution. The bacterial solution was coated on MH medium with an antibiotic table by sterile absorbent cotton at 30℃ for one day. The diameter of the bacteriostatic circle was measured and then resistance was judged. Preparation method of 0.5 M standard turbid solution: 0.0048 mol/L $BaCl_2$ 0.5 mL, 0.18 mol/L H_2SO_4 99.5 mL.

2.4. Optimal cultivation and degradation conditions of PAHs and heterocyclic derivatives

To obtain the best culture and degrading conditions, various substrates, temperatures, revolving speeds and substrate additions were performed for detection. Strain MPDS grew to the exponential phase in sterilized MSM medium (50 mL) with different substrates at 30°C and 200 rpm; the precultures of four substrates were used as seed broths (each of the seed broths was only cultured with one substrate). 4% (vol/vol) of seed broths were transferred into 50 mL MSM medium containing naphthalene (50 mg) or fluorene (2.5 mg) or DBF (2.5 mg) or DBT (2.5 mg) at various temperatures (25, 30, 37, and 42°C) with 200 rpm. To explore the appropriate revolving speed, the seed broths were transferred into MSM medium at 50, 100 and 200 rpm at an optimum temperature. In order to optimize the initial addition, the activated seed solution was transferred into 50 mL sterilized MSM with different initial concentrations (naphthalene: 0.2, 1, and 2 mg/mL; fluorene or DBF or DBT: 0.05, 0.1, 0.2, 0.4, and 1 mg/mL) at 200 rpm and 25°C. The detection of the four substrates was by HPLC and parameters were consulted from Lu's report (Lu et al., 2019), the detection wavelengths are 275 nm (naphthalene), 280 nm (DBF), 254 nm (fluorene and DBT). The standard curves were fitted by using OriginPro 9.0

156 software (Fig. S2).

157

158 *2.5. Determination of intermediates in biodegradation of naphthalene, fluorene, DBF and DBT*

159 Strain MPDS grew into the exponential phase in LB medium at optimal conditions. After
160 collected, washed and resuspended, the cells without any substrate were starved at 30°C for
161 3 hours and then diluted with PBS buffer (OD_{600} = 5.0). Four substrates were respectively added
162 into resting cell (50 mL). After ethyl acetate (50 mL) extraction, the supernatant was
163 concentrated by rotary evaporation and dissolved with 1 mL ethyl acetate, then LC-MS was used
164 to detect samples at different reaction times. The mixture of 30 μL condensed extraction and 30
165 μL BSTFA (Bis(trimethylsilyl)trifluoroacetamide, a silylation derivatization reagent) was placed
166 at 70°C for half an hour and detected by GC-MS (Liu et al., 2020). The LC-MS system (Agilent
167 6850/5975C) was as followings: the temperature of column was 30°C; flow rate was 0.4
168 mL/min; water: methanol = 20% : 80%; injection volume was 5 μL; scanning range was 190 -
169 600 nm; detection wavelengths were 275 nm (naphthalene), 280 nm (DBF), 254 nm (fluorene
170 and DBT).

171

172 *2.6. Detection of HOBB degradation by resting cells of strain MPDS*

173 A total of 0.2 mM HOBB (Liu et al., 2018) was added into resting cells of strain MPDS. The
174 colors of the supernatant between the experimental group and control group (PBS buffer with
175 0.2mM HOBB) were observed (Fig. S3C). The standard curve of HOBB (Fig. S3A) and the

176 HOBB residual at different time (Fig. S3B) was determined by HPLC (Liu et al., 2018).

177

178 *2.7. Genome sequencing and analysis*

179 The genomic DNA was extracted by Wizard genomic DNA purification kit (Promega). Illumina
180 MiSeq and PacBio sequencing platforms were used to sequence the whole genome of strain
181 MPDS (Shanghai Personalbio Technology Co., Ltd). AdapterRemoval (Schubert et al., 2016)
182 and SOAPec (Luo et al., 2012) were used to remove the joint contamination and filter the
183 low-quality reads, respectively. We used HGAP (Chin et al., 2016) and CANU (Koren et al.,
184 2017) software to assemble the data from PacBio sequencing platform to get the contig sequence.
185 The second generation of high-quality data was used to correct the third generation contig
186 results by Pilon (Walker et al., 2014). GeneMarkS (Besemer et al., 2001)
187 (http://exon.gatech.edu/GeneMark) software was used to predict protein-coding genes.
188 tRNAscan-SE (Lowe & Eddy, 1997) was used to predict tRNA, Barrnap software (0.9-dev) to
189 predict rRNA, and Rfam database (Kalvari et al., 2018) to predict other non-coding RNAs. The
190 coding-protein genes were annotated with NR (NonRedundant Protein Sequence Database),
191 KEGG (Kyoto Encyclopedia of Genes and Genomes), eggNog (Non-supervised Orthologous
192 Groups) databases and Swiss-Prot.

193

194 *2.8. Transcriptomic analysis*

195 Strain MPDS was cultured in glycerol medium (MSM+ 1% glycerol) and DBF medium (MSM

196 + 5 mg DBF), respectively. The RNA was sequenced by on Illumina sequencing platform using
197 Next-Generation Sequencing (NGS) (Shanghai Personalbio Technology Co., Ltd). Cuttadapt
198 was utilized to remove 3' joints and filter low quality reads. Bowtie2
199 (http://bowtie-bio.sourceforge.net/index.shtml) compared the filtered reads to the reference
200 genome (strain MPDS genome). Then we used Htseq 0.6.1p2
201 (http://www-huber.embl.de/users/anders/HTSeq) and DESeq (version 1.18.0) to count gene
202 expression and analyze differentially expressed genes, respectively.
203
204 *2.9. RT-qPCR analysis*
205 The RNAprep pure cell/bacteria kit (TianGen, China) was used to extract total RNA. The cDNA
206 product was obtained after DNase I (Thermo Scientific) treatment and reversed transcription
207 with Hifair Ⅱ 1st Strand cDNA Synthesis Kit (Yeasen). RT-qPCR of six genes in naphthalene
208 gene cluster and 16S gene (reference gene) was detected by quantitative PCR apparatus
209 (qTOWER^{3}G) with Hieff qPCR Green Master Mix (Yeasen) and fold change in gene expression
210 was calculated by $2^{-\Delta\Delta Ct}$ (Lu et al., 2019). The program primers of each genes are shown in
211 Table S3.
212
213 *2.10. Accession number(s)*
214 *Pseudomonas* sp. MPDS was stored in China Center for Type Culture Collection (CCTCC)
215 under accession number M 2020186. The whole-genome sequence of strain MPDS was

deposited into the NCBI database under the accession number CP054128.

3. Results

3.1. Isolation and identification of strain MPDS

A strain named MPDS efficient in degrading PAHs and heterocyclic derivatives was isolated, including naphthalene, fluorene, dibenzofuran and dibenzothiophene. The 16S rRNA gene of strain MPDS has 99% similarity sequence identity with *Pseudomonas brassicacearum*; the phylogenic tree reveals that strain MPDS is also closed to *P. brassicacearum* (Fig. 1). This identified strain MPDS has resistance to multiple antibiotics including chloramphenicol, ampicillin, and kanamycin (Table 1).

3.2. Growth conditions and degradation abilities with naphthalene, DBF, DBT and fluorene

To confirm the growth conditions and the degradation abilities of four substrates, the aerobic strain MPDS was cultured with different revolving speeds, at different temperatures and different amounts of naphthalene, fluorene, DBF and DBT. Strain MPDS hardly grew at high temperatures ($\geq$ 37℃) and the optimal growth temperature was 25℃. The growth of strain MPDS with naphthalene as a substrate at 25°C was much better than at other temperatures (Fig. S1A) while growth with fluorene, DBF or DBT at 25℃ was just slightly better than that at 30℃ (Fig. S1B-D). The optimal growth revolving speed of strain MPDS was 200 rpm (Fig. S1E-H). Because strain MPDS had a stronger capacity to degrade naphthalene, the optimal naphthalene

amount was much higher than those three substrates. When 50 mg naphthalene was added, strain MPDS grew into the logarithmic phase faster than with 100 mg, and the OD_{600} of these two amounts was basically stable at 1.0; thus, 50 mg was selected as the optimal amount of naphthalene (Fig. S1I). For fluorene, DBF and DBT, although the growth of strain MPDS was not affected by substrate addition (Fig. S1J-L), it grew better under the condition of 5 mg substrates than other amounts. The optimal temperature and flask shaking speed of growth and degradation were 25°C (Fig. S1A-D) and 200 rpm (Fig. S1E-H), respectively. The optimal amount of naphthalene was 50 mg, while 5 mg was a suitable addition amount of fluorene or DBF or DBT.

At the optimal conditions, the degradation ability of strain MPDS was tested. Strain MPDS could completely degrade 50 mg naphthalene in 84 h (Fig. 2A). A total of 65.7% DBF (5 mg in 50 mL) and 32.1% DBT (5 mg in 50 mL) could be degraded in 96 h and 40.3% fluorene (5 mg in 50 mL) could be degraded in 72 h (Fig. 2B-D).

3.3. Genomic analysis of strain MPDS

The whole genome of strain MPDS has a single circular chromosome (Fig. 3A), which contained 6,213,959 bases with the G + C content of 60.25%. Besides 5,534 protein-coding sequences, the circular chromosome contains five rRNA operons and 65 tRNA genes with the coding percentage of 87.3%.

The genes encoding the degradation of PAHs and heterocyclic aromatic hydrocarbons were

predicted on a 27,933 kbp region (Table S1). This region includes the necessary genes responsible for naphthalene degradation. The enzyme encoded by *nahAaAbAcAd* is naphthalene dioxygenase, generating cis-naphthalene dihydrodiol from naphthalene. NahA (NahAa, NahAb, NahAc, NahAd) greatly resembles their homologs in *Pseudomonas stutzeri* (sharing > 98% amino acid identity) (Bosch et al., 1999). A putative transcriptional regulator from AraC family was located upstream of *nahAa*, with 99.0% amino acid homology with the homologues in *Pseudomonas* sp. A214. The putative genes *nahBFCED* were involved in the conversion of cis-naphthalene dihydrodiol to salicylic acid (Fig. 3B), which showed high identity to their homologs in *P. stutzeri* (> 99% amino acid sequence identity) (Bosch et al., 1999) and the predicted *nahHIJKL* (Yen & Gunsalus, 1985) are genes that biodegrade salicylic acid and catechol, which have at least 98% amino acid sequence homology.

Based on genome annotation, other aromatic hydrocarbon degradation genes in this strain were also found including 4-hydroxybenzoate 3-monooxygenase, 4-hydroxyphenylacetate isomerase, and 3-phenylpropionate dioxygenase (*hcaE*). The substrates of these enzymes are mono benzene ring compounds; thus, it is speculated that they are involved in the degradation of downstream metabolites in the process of degrading PAHs. We also predicted some functional genes that are predicted to be essential for utilizing nitrate, synthesizing amino acids, transferring and absorbing C-containing compounds.

3.4. Clarification of biodegadation pathways of naphthalene, DBF, DBT and fluorene

3.4.1. The naphthalene degrading pathway

The intermediates produced during naphthalene degradation were identified by LC-MS. 1,2-dihydroxynaphthalene, salicylic acid and catechol appeared at 4.200 min, 3.152 min, and 3.834 min, respectively, and the data of *m*/*z* by the mass spectra were 159.0456 (1,2-dihydroxynaphthalene), 137.0247 (salicylic acid) and 109.0304 (catechol), respectively (Fig. 4A). Thus, we speculated that the naphthalene degradation pathway was a salicylic acid pathway (Fig. 4B). This was consistent with the degradation pathway driven by naphthalene degradation gene clusters.

3.4.2. The DBF degrading pathway

From the fermentation samples of DBF, new intermediate peaks were detected and identified, including 3-(3'-oxobenzofuran-2'-yl)propanoic acid, 2-(3'-oxobenzofuran-2'-yl) acetic acid; 2-(3'-hydroxy-2',3'-dihydrobenzofuran-2'-yl) acetic acid, 2-oxo-2-(2-hydroxyphenyl) acetic acid; 2-hydroxy-2-(2-hydroxyphenyl) acetic acid; salicylic acid; and catechol (Fig. 4F). The intermediates appeared at 4.570 min, 3.293 min, 3.742 min, 2.878 min, 2.928 min, 3.859 min and the data of m/z by mass spectra are shown in Fig. 4F. However, the most pivotal metabolite HOBB (2-hydroxy-4-(3'-oxo-3'H-benzofuran-2'-yliden) but-2-enoic acid), a yellow toxic intermediate metabolite produced during the lateral dioxygenation degradation pathway of DBF, was not identified. We then prepared HOBB (Liu et al., 2018) as the only substrate for a resting cell reaction and the results showed that strain MPDS degraded 0.2 mM HOBB in 45 h (Fig.

296 S3B-C) while many reported DBF-degrading strains had no ability to degrade HOBB efficiently
297 and rapidly. This suggested that strain MPDS could biodegrade DBF via the lateral
298 dioxygenation degradation pathway and would solve the problem in which this pathway is
299 generally interrupted by HOBB. At the same time, we used GC-MS to detect silylated salicylic
300 acid (after derivatization) at 11.097 min (Fig. 4G). The results illustrated that strain MPDS
301 possesses the lateral dioxygenation pathway of DBF with the first step of hydrolysing DBF to
302 HOBB and then degrading into salicylic acid (Fig. 4H).
303
304 *3.4.3. The DBT degrading pathway*
305 For DBT, typical products in the DBT lateral degradation pathway,
306 1,2-dihydroxydibenzothiophene, 3-hydroxy-2-formyl benzothiophene,
307 2,3-dihydroxybenzothiophene and thiosalicylic acid, were detected by LC-MS (Fig. 4I). These
308 intermediates appeared at 18.513 min, 3.018 min, 3.800 min and 2.918 min, respectively, and
309 the datas of m/z by mass spectra were 215.0176 (1,2-dihydroxydibenzothiophene), 177.0024
310 (3-hydroxy-2-formyl benzothiophene), 165.0065 (2,3-dihydroxybenzothiophene) and 153.0013
311 (thiosalicylic acid), respectively (Fig. 4I). Simultaneously, silylated thiosalicylic acid was
312 detected by GC-MS (after derivatization) at 12.692 min (Fig. 4J). These results suggested that
313 strain MPDS degraded DBT into thiosalicylic acid by the lateral dioxygenation pathway (Fig.
314 4K).
315

316 *3.4.4. The fluorene degrading pathway*

317 9-Fluorenol, 2-propanoic acid-1-indanone and 2-acetic acid-1-indanone were identified by
318 LC-MS from fluorene samples (Fig. 4C) at 7.179 min, 3.217 min and 3.217 min, respectively.
319 Moreover, we detected related metabolites of 9-fluorenone by GC-MS (after derivatization) at
320 12.951 min (Fig. 4D). 9-Fluorenol and 9-fluorenone are metabolites in the angular
321 dioxygenation pathway; 2-propanoic acid-1-indanone and 2-acetic acid-1-indanone belong to
322 the lateral dioxygenation pathway. Thus, we inferred that strain MPDS might contain both
323 angular and lateral dioxygenation pathways (Fig. 4E) but the metabolic pathway of fluorene
324 degradation remains to be further studied.

325 In summary, biodegradation of DBF, DBT and fluorene is via the lateral dioxygenation
326 pathways in strain MPDS, which is usually found in co-metabolism strains. We did not find
327 similar reported genes for degradation of DBF, DBT or fluorene in the genome of strain MPDS.
328 Therefore, we inferred that strain MPDS may carry new metabolic gene clusters of the lateral
329 dioxygenation pathways for DBF, DBT and fluorene degradation.

330

331 *3.5. Transcriptional analysis*

332 In order to search for potential degradation gene clusters, we performed transcriptome analysis.
333 In view of physiological and biochemical properties, strain MPDS has a stronger ability to
334 degrade DBF than DBT or fluorene. Therefore, we chose DBF as the substrate for transcriptome
335 data analysis to search for functional genes. According to the transcriptome results, 870 genes

show differential expression levels between the negative control group (cultured by 1% glycerol) and experimental group (cultured by DBF). On the conditions of log2|fold change|>1 and P-values <0.05, 487 genes were up-regulated and 383 genes were down-regulated (Fig. 5A and D). Genes with similar expression levels were identified by cluster analysis (Fig. 5B). The enrichment analysis of KEGG pathway found that differentially expressed genes were mainly related to the degradation of valine, leucine and isoleucine, the metabolism of glyoxylate and dicarboxylate, and the metabolic pathway of propanoate (Fig. 5C).

The initial genes encoding the enzyme (NahA) of the naphthalene degradation pathway were up-regulated induced with DBF or its intermediates, and the gene encoding salicylaldehyde dehydrogenase was also highly expressed. Moreover, quantities of other predicted genes might play significant roles during DBF degradation were also up-regulated, such as the coding genes of 4-hydroxybenzoate 3-monooxygenase, 4-hydroxyphenylacetate isomerase, and 3-phenylpropionate dioxygenase (*hcaE*). We also found 107 potential and unknown-function genes, which were up-regulated and might be essential to DBF degradation, were deserved further attention. However, we did not find any genes sharing high similarity with the reported DBF-degrading genes, which indicated that there would be novel DBF-degrading genes of unknown function in those up-regulated gene clusters, such as the putative protein genes in the vicinity of *nahAFBCED*, the upstream or downstream hypothetical protein genes of monophenyl compound metabolism genes and other clusters of hypothetical protein genes with unknown functions.

356

357 *3.6. Comparative genomic analysis of DBF degradation strains*

358 In a previous study, we isolated and reported on another DBF-degrading *Pseudomonas* sp. strain
359 FA-HZ1 (Ali et al., 2019). To obtain comprehensive information of the DBF-degrading pathway
360 in strain MPDS and to screen more potential functional genes, we analyzed the genomic
361 sequences of these two strains together. These two strains showed high sequence identity (more
362 than 80%) in 249 genes. Most of them are responsible for basic metabolism activities, including
363 DNA replication and repair, transcription regulatory factors, ribosomal protein synthesis, amino
364 acid degradation and transport, aldehyde dehydrogenase, carbohydrate metabolism enzymes and
365 so on. In addition to these genes with clear functions, we also found 13 genes with highly
366 similar sequences that were up-regulated in transcriptome data of strain MPDS (Table S2 and
367 Fig. 6). Particularly, we found that the expression of a hypothetical protein (gene 4284), which
368 was downstream of the naphthalene degradation gene cluster, was up-regulated by 7.8 times and
369 there were seven up-regulated genes nearby.

370

371 *3.7. Real-time quantitative PCR (RT-qPCR) of naphthalene gene cluster*

372 We found a naphthalene-degrading gene cluster in strain MPDS, according to genomic data and
373 transcriptome data growing with DBF, and the expression of *nahAa*, *nahAb* and *nahAc*, which
374 encode naphthalene 1,2-dioxygenase, was up-regulated. To determine the role of this gene
375 cluster in naphthalene degradation, we performed real-time quantitative PCR of 16S rRNA gene

(reference gene) and six genes (*nahA, nahB*, *nahD, nahF, nahH* and *nahO*), which located upstream or downstream of naphthalene degradation gene cluster (Fig. 7). The expression of *nahA* and *nahB* that encoded naphthalene dioxygenase and dehydrogenase were highly up-regulated by 37.8 times and 42.2 times compared with control group (glycerol). These two genes are initial and pivotal in naphthalene degradation and degrade naphthalene into 1,2-dihydroxynaphthalene. Another high expression gene *nahH*, which encoded catechol 2,3-dioxygenase, was up-regulated by 36.1 times. However, other three genes (*nahF*, *nahD*, and *nahO*) did not show up-regulated evidently, which could encode salicylaldehyde dehydrogenase, 2-hydroxychromene-2-carboxylate isomerase and acetaldehyde dehydrogenase.

The RT-qPCR results suggest that express of some genes in the naphthalene gene cluster of strain MPDS might be induced by naphthalene or its intermediate metabolites, but some of them were constitutive expression. The regulatory mechanism of naphthalene degradation in strain MPDS needs further exploration.

4. Discussion

There are many reports about degradation strains of naphthalene, fluorene, DBF and DBT. *Pseudomonas* (Bosch et al., 1999; Yen & Gunsalus, 1985; Ali et al., 2019), *Rhodococcus* (Andreoni et al., 2000), *Micrococcus* (Wen et al., 2006), *Alcaligenes* (Guerin & Boyd, 1995) and *Corynebacterium* can degrade naphthalene. Besides *Pseudomonas* and *Rhodococcus*, there are several microorganisms that can utilize fluorene, DBF or DBT, including *Sphingomonas* (Wilkes et al., 1996; Gai et al., 2007), *Burkholderia* (Gregorio et al., 2004), *Rhizobium meliloti*

(Frassinetti et al., 1998), *Terrabacter* (Schmid et al., 1997; Kasuga et al., 2013) and so on. Many researchers have studied the angular dioxygenation pathway and lateral dioxygenation pathway of fluorene, DBF or DBT and several pivotal genes in angular dioxygenation pathway have been reported while genes in the lateral dioxygenation pathway remained to be discovered. The lateral degradation pathway of DBF and DBT is mainly through co-metabolism. For example, Stope et al. (2002) found that *Rhodococcus erythropolis* SBUG 271 cultured with biphenyl could co-metabolize DBF. Seo et al. (2006) isolated *Arthrobacter* sp. P1-1 that co-metabolized DBT with phenanthrene. These strains are incapable of utilizing DBF or DBT independently, thus, specific genes involved in this pathway have not been reported. On the other hand, theses degradation pathways by co-metabolizing microorganisms are usually blocked at a certain step. For example, DBF degradation is generally interrupted due to toxic product HOBB, while DBT-degrading strains usually cannot fully desulfurize DBT, resulting in the accumulation of 3-hydroxy-2-formyl benzothiophene. Therefore, it is a significant advantage that strain MPDS can degrade naphthalene, fluorene, DBF and DBT, which is rare in past studies. Moreover, the reported genes have not been found in the strain MPDS genome, which suggests that strain MPDS might carry novel functional genes of PAHs degradation, and deserves further study.

The degradation genes of naphthalene in *P. putida* G7, *P. putida* NICB9816 (Simon et al., 1993) and *P. stutzeri* AN10 (Bosch et al., 1999) were studied in detail. The degradation genes were found both on plasmids and chromosomes in different strains. For example, gene cluster *nahAaAbAcAdBFCED* of *P. stutzeri* AN10 are distributed on chromosomes, and the

naphthalene-degrading genes from *P. putida* G7 are on NAH7 plasmid. Notably, NAH7 plasmid from *P. putida* G7 contains two different gene degradation pathway clusters. The first gene cluster is *nahAaAbAcAdBFCED* that degrade naphthalene into salicylic acid and another gene cluster *nahGHILJKMNOR* completely biodegraded via catechol. Besides the catechol pathway, there is a gentianic acid pathway in naphthalene degradation. The beginning of another degradation pathway is as the same as the first one, while the second part of the pathway is via gentianic acid not catechol. The researchers also found other highly conserved naphthalene-degrading gene clusters, such as NAH-like gene cluster, *pah* gene cluster of *P. putida* ous82, *nah* gene cluster on pDTG1 from *P. putida* NICB9816-4 and *dox* gene cluster on C18 plasmid of *Pseudomonas* C18 (Kiyohara et al., 1994; Dennis & Zylstra, 2004; Takizawa et al., 1999). For strain MPDS, *nahAaAbAcAdBFCED* was identified clearly, and is highly similar to the gene cluster of *P. stuttzeri* (sequence homology > 98%). In addition, we found a catechol degradation gene near the naphthalene gene cluster in strain MPDS. Thus we suggest that the degradation is via salicylic acid pathway.

To obtain a comprehensive information of the DBF-degrading pathway in strain MPDS and screen more potential functional genes, we analyzed the genomic sequences of strain MPDS along with strain FA-HZ1 (Ali et al., 2019). These two strains showed high sequence identity (more than 80%) in 249 genes and 13 of these genes were up-regulated in transcriptome data of strain MPDS (Table S2 and Fig. 6). Particularly, we found that the expression of a hypothetical protein (gene 4284), which was downstream of the naphthalene degradation gene cluster, was

436 up-regulated by 7.8 times and there were seven up-regulated genes nearby. These unknown
437 genes might be related to the degradation of DBF and deserve further study.

438 In summary, the *Pseudomonas* strain MPDS is able to utilize naphthalene, fluorene, and
439 their heterocyclic derivatives DBF and DBT as the only carbon sources for growth, and could
440 biodegrade fluorene, DBF, and DBT via lateral dioxygenation metabolic pathways, which are
441 rare in previous studies. Considering the lack of molecular mechanisms and biochemical
442 properties of the lateral dioxygenation pathways of fluorene, DBF, and DBT, strain MPDS could
443 be a significant microbial resource in degrading PAHs. We determined the degradation ability of
444 strain MPDS, clarified the degradation pathways of four substrates, identified the functional
445 genes of naphthalene degradation, and analyzed genomic sequences and transcriptome data of
446 potential genes. In further research, we will exploit novel genes of the lateral dioxygenation
447 metabolic pathways of fluorene, DBF and DBT degradation, and give more information about
448 molecular mechanisms of lateral dioxygenation metabolic pathways. Such work will benefit the
449 bioremediation of sites contaminated by PAHs and heterocyclic aromatics.

450

451 **CRediT authorship contribution statement**

452 YL liu, and HY Hu performed the experiments. HZ Tang and HY Hu designed the experiments.
453 YL liu, HY Hu and HZ Tang wrote the manuscript. P Xu, HZ Tang and Giulio Zanaroli revised
454 the manuscript. P Xu and HZ Tang conceived the project.

455 **Declaration of Competing Interest**

None.

Acknowledgments

This study was supported by the grants from Science and Technology Commission of Shanghai Municipality (17JC1403300), from Shanghai Excellent Academic Leaders Program (20XD1421900), from the National Key Research and Development Project (2018YFA0901200). We acknowledge the 'Shuguang Program' (17SG09) supported by Shanghai Education Development Foundation and Shanghai Municipal Education Commission. Thanks to the Shanghai Personal Biotechnology Co., Ltd for genome and transcriptome sequencing.

References

Aly, H. A. H., Huu, N. B., Wray, V., Junca, H., and Pieper, D. H., 2008. Two angular dioxygenases contribute to the metabolic versatility of dibenzofuran-degrading *Rhodococcus* sp. strain HA01. *Appl. Environ. Microbiol.* 74(12), 3812–3822.

Ali, F., Hu, H. Y., Wang, W. W., Zhou, Z. K., Shah, S. B., Xu, P., and Tang, H. Z., 2019. Characterization of a dibenzofuran-degrading strain of *Pseudomonas aeruginosa*, FA-HZ1. *Environ. Pollut*. 250, 262–273.

Andreoni, V., Bernasconi, S., Colombo, M., Beilen, J. B. V., and Cavalca, L., 2000. Detection of genes for alkane and naphthalene catabolism in *Rhodococcus* sp. strain 1BN. *Environ. Microbiol.* 2(5), 572–577.

Becher, D., Specht, M., Hammer, E., Francke, W., and Schauer, F., 2000. Cometabolic degradation of dibenzofuran by biphenyl-cultivated *Ralstonia* sp. strain SBUG 290. *Appl. Environ. Microbiol*. 66(10), 4528–4531.

Bosch, R., Garcia-Valdes, E., and Moore, E. R., 1999. Genetic characterization and evolutionary implications of a chromosomally encoded naphthalene-degradation upper pathway from *Pseudomonas stutzeri* AN10. *Gene* 236(1), 149–157.

Besemer, J., Lomsadze, A., and Borodovsky, M., 2001. GeneMarkS: a self-training method for prediction of gene starts in microbial genomes. Implications for finding sequence motifs in regulatory regions. *Nucleic Acids Res*. 29(12), 2607–2618.

Casellas, M., Grifoll, M., Bayona, J. M., and Solanas, A. M., 1997. New metabolites in the degradation of fluorene by *Arthrobacter* sp. strain F101. *Appl. Environ. Microbiol.* 63(3), 819–826.

Chin, C. S., Peluso, P., Sedlazeck, F. J., Nattestad, M., Concepcion, G. T., Clum, A., Dunn, C., O'Malley, R., Figueroa-Balderas, R., Morales-Cruz, A., Cramer, G. R., Delledonne, M., Luo, C. Y., Ecker, J. R., Cantu, D., Rank, D. R., and Schatz, M. C., 2016. Phased diploid genome assembly with single-molecule real-time sequencing. *Nat Methods* 13(12), 1050–1054.

Dennis, J. J., and Zylstra, G. J., 2004. Complete sequence and genetic organization of pDTG1, the 83 kilobase naphthalene degradation plasmid from *Pseudomonas putida* strain NCIB 9816-4. *J. Mol. Biol*. 341(3), 753–768.

Gregorio, S. D., Zocca, C., Sidler, S., Toffanin, A., Lizzari, D., and Vallini, G., 2004. Identification of two new sets of genes for dibenzothiophene transformation in *Burkholderia* sp. DBT1. *Biodegradation* 15(2), 111–123.

Fortnagel, P., Harms, H., Wittich, R. M., Krohn, S., Meyer, H., Sinnwell, V., Wilkes, H., and Francke, W., 1990. Metabolism of dibenzofuran by *Pseudomonas* sp. strain hh69 and the mixed culture hh27. *Appl. Environ. Microbiol.* 56(4), 1148–1156.

Frassinetti, S., Setti, L., Corti, A., Farrinelli, P., Montevecchi, P., and Vallini, G., 1998. Biodegradation of dibenzothiophene by a nodulating isolate of *Rhizobium meliloti*. *Can. J. Microbiol*. 44(3), 289–297.

Grifoll, M., Selifonov, S. A., Gatlin, C. V., and Chapman, P. J., 1995. Actions of a versatile fluorene-degrading bacterial isolate on polycyclic aromatic compounds. *Appl. Environ.*

Microbiol. 61(10), 3711–3723.
Gai, Z. H., Yu, B., Li, L., Wang, Y., Ma, C. Q., Feng, J. H., Deng, Z. X., and Xu, P., 2007. Cometabolic degradation of dibenzofuran and dibenzothiophene by a newly isolated carbazole-degrading *Sphingomonas* sp. strain. *Appl. Environ. Microbiol.* 73(9), 2832–2838.
Guerin, W. F., and Boyd, S. A., 1995. Maintenance and induction of naphthalene degradation activity in *Pseudomonas putida* and an *Alcaligenes* sp. under different culture conditions. *Appl. Environ. Microbiol*. 61(11), 4061–4068.
Haritash, A. K., and Kaushik, C. P., 2009. Biodegradation aspects of polycyclic aromatic hydrocarbons (PAHs): A review. *J. Hazard. Mater*. 169(1-3), 1–15.
Ji, X. Y., Xu, J., Ning, S. X., Li, N., Tan, L., and Shi, S. N., 2017. Cometabolic degradation of dibenzofuran and dibenzothiophene by a naphthalene-degrading *Comamonas* sp. JB. *Curr. Microbiol*. 74(12), 1411–1416.
Kasuga, K., Nitta, A., Kobayashi, M., Habe, H., Nojiri, H., Yamane, H., Omori, T., and Kojima, I., 2013. Cloning of *dfdA* genes from *Terrabacter* sp. strain DBF63 encoding dibenzofuran 4,4a-dioxygenase and heterologous expression in *Streptomyces lividans*. *Appl. Microbiol. Biotechnol*. 97(10), 4485–4498.
Kalvari, I., Argasinska, J., Quinones-Olvera, N., Nawrocki, E. P., Rivas, E., Eddy, S. R., Bateman, A., Finn, R. D., Petrov, A. I., 2018. Rfam 13.0: Shifting to a genome-centric resource for non-coding RNA families. *Nucleic Acids Res.* 46(D1), D335–D342.
Kiyohara, H., Torigoe, S., Kaida, N., Asaki, T., Iida, T., Hayashi, H., and Takizawa, N., 1994. Cloning and characterization of a chromosomal gene cluster, *pah*, that encodes the upper pathway for phenanthrene and naphthalene utilization by *Pseudomonas putida* OUS82. *J. Bacteriol*. 176(8), 2439–2443.
Koren, S., Walenz, B. P., Berlin, K., Miller, J. R., Bergman, N. H., and Phillippy, A. M., 2017. Canu: scalable and accurate long-read assembly via adaptive k-mer weighting and repeat separation. *Genome Res.* 27(5), 722–736.
Li, Q. G., Wang, X. Y., Yin, G.B., Gai, Z. H., Tang, H. Z., Ma, C. Q., Deng, Z. X., and Xu, P., 2009. New metabolites in dibenzofuran cometabolic degradation by a biphenyl-cultivated *Pseudomonas putida* strain B6-2. *Environ. Sci. Technol*. 43(22), 8635–8642.
Luo, R. B., Liu, B. H., Xie, Y. L., Li, Z. Y., Huang, W. H., Yuan, J. Y., He, G. Z., Chen, Y. X., Pan, Q., Liu, Y. J., Tang, J. B., Wu, G. X., Zhang, H., Shi, Y. J., Liu, Y., Yu, C., Wang, B., Lu, Y., Han, C. L., Cheung, D.W., Yiu, S. M., Peng, S. L., Zhu, X. Q., Liu, G. M., Liao, X. K., Li, Y. R., Yang, H. M., Wang, J., Lam, T. W., and Wang, J., 2012. SOAPdenovo2: an empirically improved memory-efficient short-read de novo assembler. *GigaScience.* 1(1), 18–18.
Lu, X. Y., Wang, W. W., Zhang, L. G., Hu, H. Y., Xu, P., Wei, T., Tang, H. Z., 2019. Molecular mechanism of N, N-dimethylformamide degradation in Methylobacterium sp. strain DM1. *Appl. Environ. Microbiol.* 85(12), e00275-19.
Liu Y. F., Wang W. W., Shah, S. B., Zanaroli, G., Xu P., and Tang H. Z., 2020. Phenol biodegradation by *Acinetobacter radioresistens* APH1 and its application in soil bioremediation. *Appl. Microbiol. Biotechnol.* 2020, 104(1), 427–437.
Liu X., Wang W. W., Hu H. Y., Lu X. Y., Zhang L. G., Xu P., and Tang H. Z., 2018.

2-Hydroxy-4-(3′-oxo-3′ H-benzofuran-2′-yliden) but-2-enoic acid biosynthesis from dibenzofuran using lateral dioxygenation in a *Pseudomonas putida* strain B6-2 (DSM 28064). *Bioresour. Bioprocess*. 5, 23.

Lowe, T. M., and Eddy, S. R., 1997. tRNAscan-SE: A program for improved detection of transfer RNA genes in genomic sequence. *Nucleic Acids Res.* 25(5), 955–964.

Nojiri, H., Kamakura, M., Urata, M., Tanaka, T., Chung, J. S., Takemura, T., Yoshida, T., Habe, H., and Omori, T., 2002. Dioxin catabolic genes are dispersed on the *Terrabacter* sp. DBF63 genome. *Biochem. Biophys. Res. Commun*. 296(2), 233–240.

Nojiri, H., Habe, H., and Omori, T., 2001. Bacterial degradation of aromatic compounds via angular dioxygenation. *J. Gen. Appl. Microbiol*. 47(6), 279–305.

Takizawa, N., Iida, T., Sawada, T., Yamauchi, K., Wang, Y. W., Fukuda. M., and Kiyohara, H., 1999. Nucleotide sequence and characterization of genes encoding naphthalene upper-pathway of *Pseudomonas aeruginosa* PAK1 and *P. putida* OUS82. *J. Biosci. Bioeng*. 87(6), 721–731.

Oldfield, C., Pogrebinsky, O., Simmonds, J., Olson, E. S., and Kulpa, C. F., 1997. Elucidation of the metabolic pathway for dibenzothiophene desulphurization by *Rhodococcus* sp. strain IGTS8 (ATCC 53968). *Microbiology* 143(Pt 9), 2961–2973.

Sakshi, Singh, S. K., and Haritash, A. K., 2019. Polycyclic aromatic hydrocarbons: soil pollution and remediation. *Int. J. Environ. Sci. Te.* 16(10), 6489–6512.

Sakshi, and Haritash, A. K., 2020. A comprehensive review of metabolic and genomic aspects of PAH-degradation. *Arch. Microbiol.* doi: 10.1007/s00203-020-01929-5.

Schmid, A., Rothe, B., Altenbuchner, J., Ludwig, W., and Engesser, K. H., 1997. Characterization of three distinct extradiol dioxygenases involved in mineralization of dibenzofuran by *Terrabacter* sp. strain DPO360. *J. Bacteriol.* 179(1), 53–62.

Seo, J. S., Keum, Y. S., Cho, I. K., and Li, Q. X., 2006. Degradation of dibenzothiophene and carbazole by *Arthrobacter* sp. P1-1. *Int. Biodeter. Biodegr.* 58(1), 36–43.

Shi, S. N., Zhang, X. W., Ma, F., Sun, T. H., Li, A., Zhou, J. T., and Qu, Y. Y., 2013. Cometabolic degradation of dibenzofuran by *Comamonas* sp. MQ. *Process Biochem.* 48(10), 1553–1558.

Sukda, P., Gouda, N., Ito, E., Miyauchi, K., Masai, E., and Fukuda, M., 2009. Characterization of a transcriptional regulatory gene involved in dibenzofuran degradation by *Nocardioides* sp. Strain DF412. *Biosci. Biotechnol. Biochem.* 73(3), 508–516.

Stope, M.B., Becher, D., Hammer, E., and Schauer, F., 2002. Cometabolic ring fission of dibenzofuran by Gram-negative and Gram-positive biphenyl-utilizing bacteria. *Appl. Microbiol. Biotechnol.* 59(1), 62–67.

Simon, M. J., Osslund, T. D., Saunders, R., Ensley, B. D., Suggs, S., Harcourt, A., Suen, W.C., Cruder, D.L., Gibson, D.T., and Zylstra, G.J., 1993. Sequences of genes encoding naphthalene dioxygenase in *Pseudomonas putida* strains G7 and NCIB 9816-4. *Gene* 127(1), 31–37.

Schubert, M., Lindgreen, S., and Orlando, L., 2016. AdapterRemoval v2: rapid adapter trimming, identification, and read merging. *BMC Res. Notes* 9, 88–88.

588 Schuler, L., Chadhain, S. M. N., Jouanneau, Y., Meyer, C., Zylstra, G. J., Hols, P., and Agathos,
589 S. N., 2008. Characterization of a novel angular dioxygenase from fluorene-degrading
590 *Spingomonas* sp strain LB126. *Appl. Environ. Microbiol.* 74(4), 1050–1057.
591 Trenz, S. P., Engesser, K. H., Fischer, P., and Knackmuss, H., 1994. Degradation of fluorene by
592 *Brevibacterium* sp. strain DPO 1361: a novel C-C bond cleavage mechanism via
593 1,10-dihydro-1,10-dihydroxyfluoren-9-one. *J. Bacteriol.* 176(3), 789–795.
594 Wilkes, H., Wittich, R., Timmis K. N., Fortnagel, P., and Francke, W., 1996. Degradation of
595 chlorinated dibenzofurans and dibenzo-pdioxins by *Sphingomonas* sp. strain RW1. *Appl.*
596 *Environ. Microbiol.* 62(2), 367–371.
597 Wattiau, P., Bastiaens, L., Herwijnen, R. V., Daal, L., Parsons, J. R., Renard, M. E., Springael,
598 D., and Cornelis, G.R., 2001. Fluorene degradation by *Sphingomonas* sp. LB126 proceeds
599 through protocatechuic acid: a genetic analysis. *Res. Microbiol.* 152(10), 861–872.
600 Walker, B. J., Abeel, T., Shea, T., Priest, M., Abouelliel, A., Sakthikumar, S., Cuomo, C. A.,
601 Zeng, Q. D., Wortman, J., Young, S. K., and Earl, A. M., 2014. Pilon: an integrated tool for
602 comprehensive microbial variant detection and genome assembly improvement. *PLoS One*
603 9(11), e112963.
604 Wen, H. Y., Liao Y. Z., and Li, X.D., 2006. Degradation characteristics of naphthalene by strain
605 N-1. *Chin. J. Appl. Environ. Biol.* 12(1), 96–98.
606 Xu, S. S., Liu, W. W., and Tao, S., 2006. Emission of polycyclic aromatic hydrocarbons in China.
607 *Environ. Sci. Technol.* 40(3), 702–708.
608 Yen, K. M., and Gunsalus, I. C., 1985. Regulation of naphthalene catabolic genes of plasmid
609 NAH7. *J. Bacteriol.* 162(3), 1008–1013.
610 Zhang, Y. X., Dou, H., Chang, B., Wei, Z. C., Qiu, W. X., Liu, S. Z., Liu, W. X., and Tao, S.,
611 2008. Emission of polycyclic aromatic hydrocarbons from indoor straw burning and
612 emission inventory updating in China. *Ann. Ny. Acad. Sci.* 1140, 218–227.

Figure legends

Fig. 1. Phylogenetic relationships of strain MPDS. Neighbor-Joining phylogenetic tree of 16S rRNA sequences of strain MPDS, with 1,000 bootstrap replications, is shown. The accession numbers in phylogenetic tree are from NCBI database and RDP database. The strains with "T" are type bacteria. The phylogenetic tree revealed that strain MPDS is closed to *Pseudomonas brassicacearum.*

Fig. 2. Degradation abilities of strain MPDS cultured with naphthalene (A), fluorene (B), DBF (C) and DBT (D) under optimal growth conditions. CK：MSM without strain MPDS. EG: MSM with strain MPDS.

Fig. 3. Genomic analysis of strain MPDS. (A) Genome map. From inside to outside, circle 1 is scale; circle 2 is G + C skew; circle 3 is the content of G + C; circles 4 and 7 are clusters of orthologous groups; circles 5 and 6 are locations of coding sequence, tRNA, and rRNA genes. (B) Predicted naphthalene degradation gene cluster in strain MPDS. Genes with different color represent different functions (blue, naphthalene hydrolysis; yellow, salicylic acid degradation). The sizes and directions of arrows indicate the sizes and transcription direction of genes. The genes are summarized in Table S1. (C) Reported naphthalene degradation gene clusters. (Gray, naphthalene-degradation gene cluster from plasmid NAH7 in *Pseudomonas putida* G7; orange, *dox* gene cluster on C18 plasmid of *Pseudomonas* C18; pink, naphthalene-degradation gene cluster from *Pseudomonas stutzeri* AN10).

Fig. 4. Pathways proposed for the degradation and identification of intermediates of naphthalene, DBF, DBT and fluorene by strain MPDS. (A) LC-MS mass spectra of naphthalene derivatives: 1,2-dihydroxynaphthalene (II), salicylic acid (V), catechol VI). (B) Proposed dioxygenation pathway of naphthalene. (C) LC-MS mass spectra of fluorene derivatives: 9-fluorenol (I), 2-Propanoic acid-1-indanone (IV) and 2-acetic acid-1-indanone (V). (D)GC-MS mass spectra of fluorene derivative: 9-fluorenone (II). (E) Proposed lateral dioxygenation pathway of fluorene. (F) LC-MS mass spectra of DBF derivatives: 3-(3′-oxobenzofuran-2′-yl)propanoic acid (III), 2-(3′-oxobenzofuran-2′-yl)acetic acid (IV), 2-(3′-hydroxy-2′,3′-dihydrobenzofuran-2′-yl)acetic acid (V), 2-oxo-2-(2-hydroxyphenyl)acetic acid (VI), salicylic acid (VII) and catechol (VIII). (G)GC-MS mass spectra of DBF derivative: silylation salicylic acid (VIII). (H) Proposed lateral dioxygenation pathway of DBF. (I) LC-MS mass spectra of DBT derivatives: 1,2-dihydroxydibenzothiophene (I), 3-hydroxy-2-formyl-benzothiophene (III), 2,3-dihydroxybenzothiophene (IV) and thiosalicylic acid (V). (J) GC-MS mass spectra of DBT derivative: silanized thiosalicylic acid (V). (K) Proposed lateral dioxygenation pathway of DBT.

Fig. 5. Transcriptome analysis in strain MPDS induced by DBF. (A) The numbers of genes which were up-regulated or down-regulated induced with DBF. (B) Hierarchical cluster heat map of gene expression in strain MPDS. DBF, experimental group cultured with DBF; CK, control group cultured with glycerol. (C) The enrichment analysis of KEGG pathways of differentially expressed genes induced with DBF. (D) Volcano Plot. The abscissa is the value of log2 of fold change. The ordinate is the value of -log10 of p-value. In this Figure, the vertical

652 line represents 2-fold change threshold; the horizontal line represents the p-value of 0.05. Every
653 gene is represented by a point, red points represent up-regulated genes while blue points
654 represent down-regulated genes, gray points represent nonsignificant differentially expressed
655 genes.

656 **Fig. 6.** Up-regulated genes in strain MPDS induced with DBF that have high sequence identity
657 (more than 80%) with strain FA-HZ1.

658 **Fig. 7.** RT-qPCR of genes related to degrading naphthalene in strain MPDS; 16S rRNA was
659 regarded as a reference gene. Different colors of bars represent different functional genes.
660 Experience group: 50 mg naphthalene induction; control group: 1% glycerol.

Fig. 1

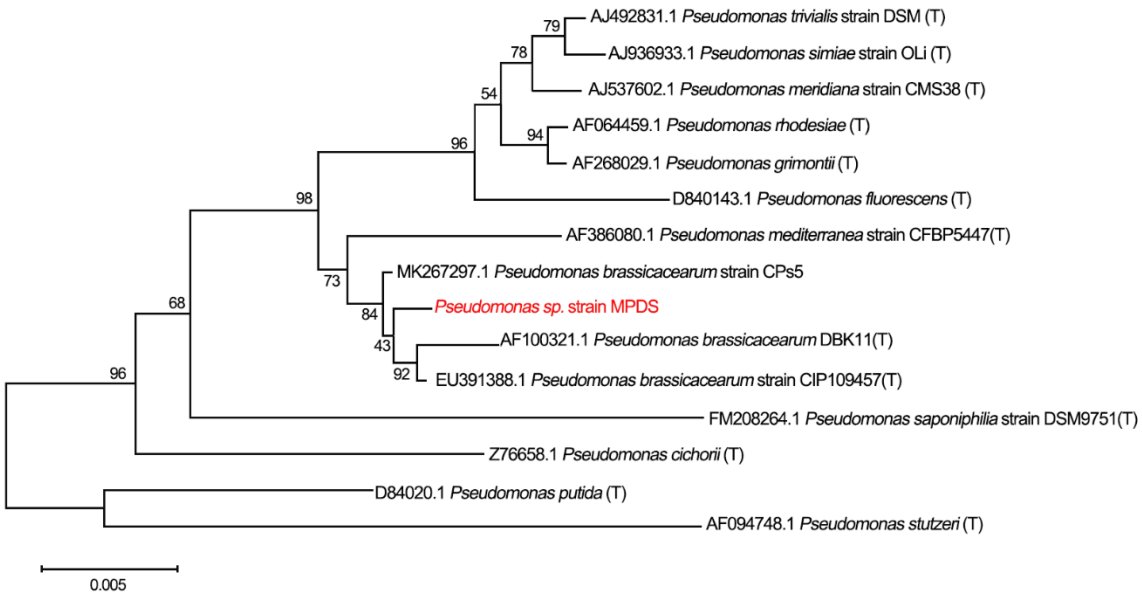
AJ492831.1 Pseudomonas trivialis strain DSM (T)
AJ936933.1 Pseudomonas simiae strain OLi (T)
AJ537602.1 Pseudomonas meridiana strain CMS38 (T)
AF064459.1 Pseudomonas rhodesiae (T)
AF268029.1 Pseudomonas grimontii (T)
D840143.1 Pseudomonas fluorescens (T)
AF386080.1 Pseudomonas mediterranea strain CFBP5447(T)
MK267297.1 Pseudomonas brassicacearum strain CPs5
Pseudomonas sp. strain MPDS
AF100321.1 Pseudomonas brassicacearum DBK11(T)
EU391388.1 Pseudomonas brassicacearum strain CIP109457(T)
FM208264.1 Pseudomonas saponiphilia strain DSM9751(T)
Z76658.1 Pseudomonas cichorii (T)
D84020.1 Pseudomonas putida (T)
AF094748.1 Pseudomonas stutzeri (T)
79
78
54
94
96
98
73
84
43
92
68
96
0.005

Fig. 2

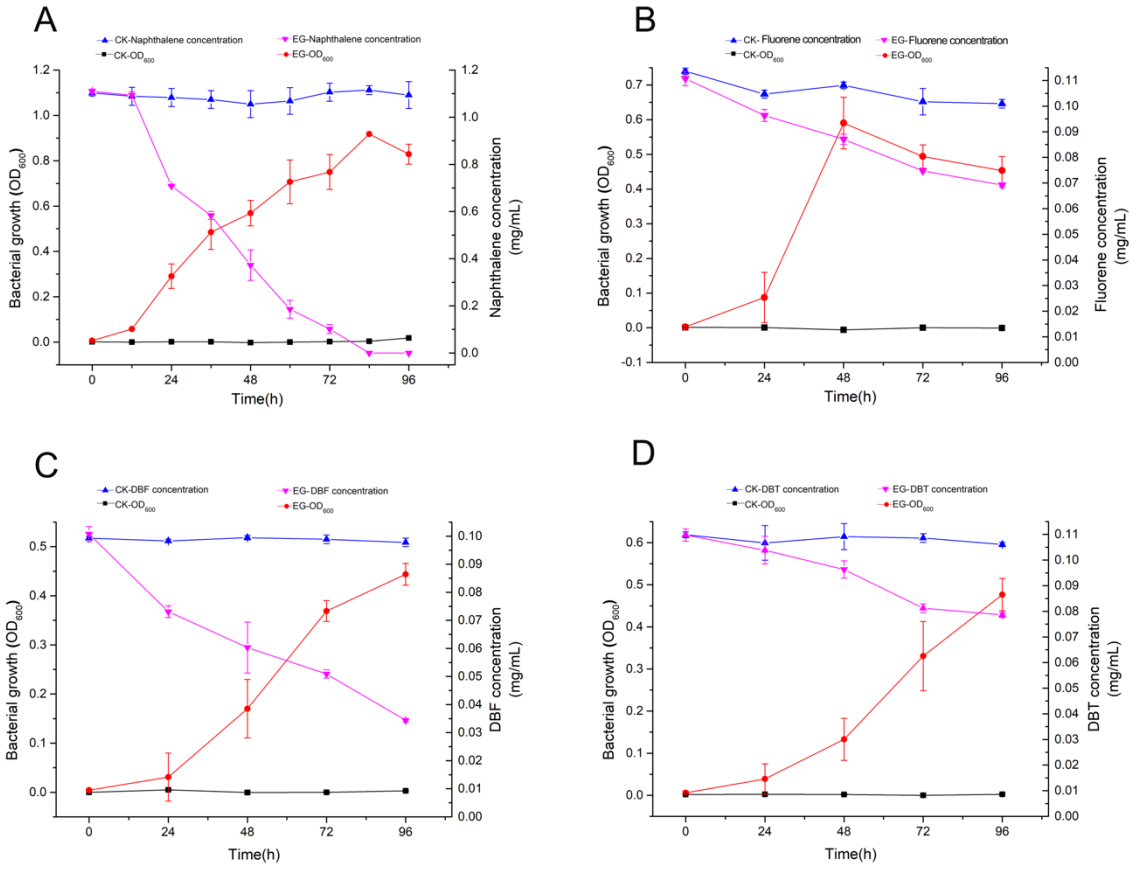
A
CK-Naphthalene concentration
EG-Naphthalene concentration
CK-OD600
EG-OD600
Bacterial growth (OD600)
Naphthalene concentration (mg/mL)
Time(h)
B
CK- Fluorene concentration
EG-Fluorene concentration
CK-OD600
EG-OD600
Bacterial growth (OD600)
Fluorene concentration (mg/mL)
Time(h)
C
CK-DBF concentration
EG-DBF concentration
CK-OD600
EG-OD600
Bacterial growth (OD600)
DBF concentration (mg/mL)
Time(h)
D
CK-DBT concentration
EG-DBT concentration
CK-OD600
EG-OD600
Bacterial growth (OD600)
DBT concentration (mg/mL)
Time(h)

Fig. 3

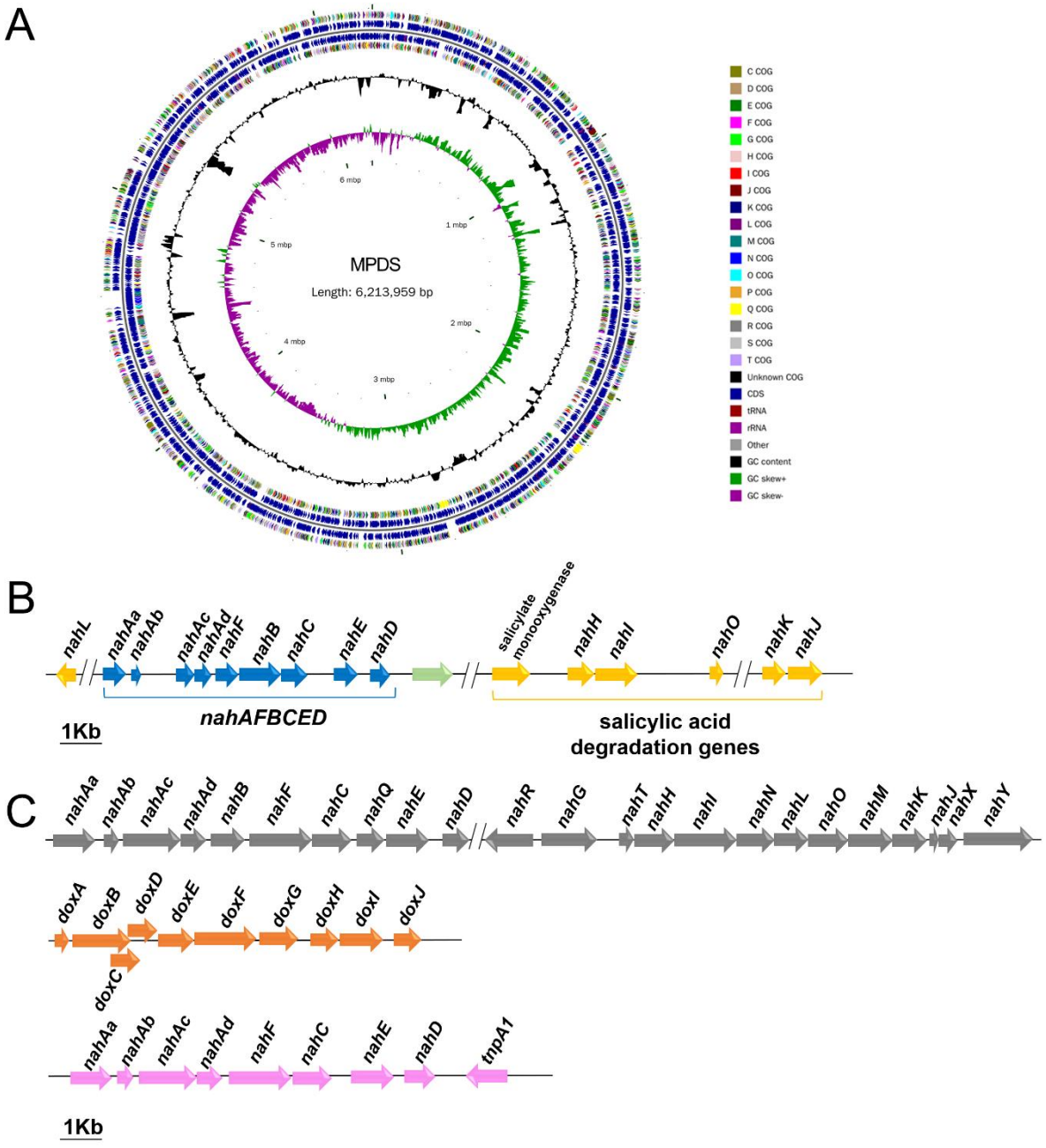
A
MPDS
Length: 6,213,959 bp
1 mbp
2 mbp
3 mbp
4 mbp
5 mbp
6 mbp
C COG
D COG
E COG
F COG
G COG
H COG
I COG
J COG
K COG
L COG
M COG
N COG
O COG
P COG
Q COG
R COG
S COG
T COG
Unknown COG
CDS
tRNA
rRNA
Other
GC content
GC skew+
GC skew-
B
nahL
nahAa
nahAb
nahAc
nahAd
nahF
nahB
nahC
nahE
nahD
salicylate monooxygenase
nahH
nahI
nahO
nahK
nahJ
nahAFBCED
salicylic acid degradation genes
1Kb
C
nahAa
nahAb
nahAc
nahAd
nahB
nahF
nahC
nahQ
nahE
nahD
nahR
nahG
nahT
nahH
nahI
nahN
nahL
nahO
nahM
nahK
nahJ
nahX
nahY
doxA
doxB
doxD
doxE
doxF
doxG
doxH
doxI
doxJ
doxC
nahAa
nahAb
nahAc
nahAd
nahF
nahC
nahE
nahD
tnpA1
1Kb

Fig. 4

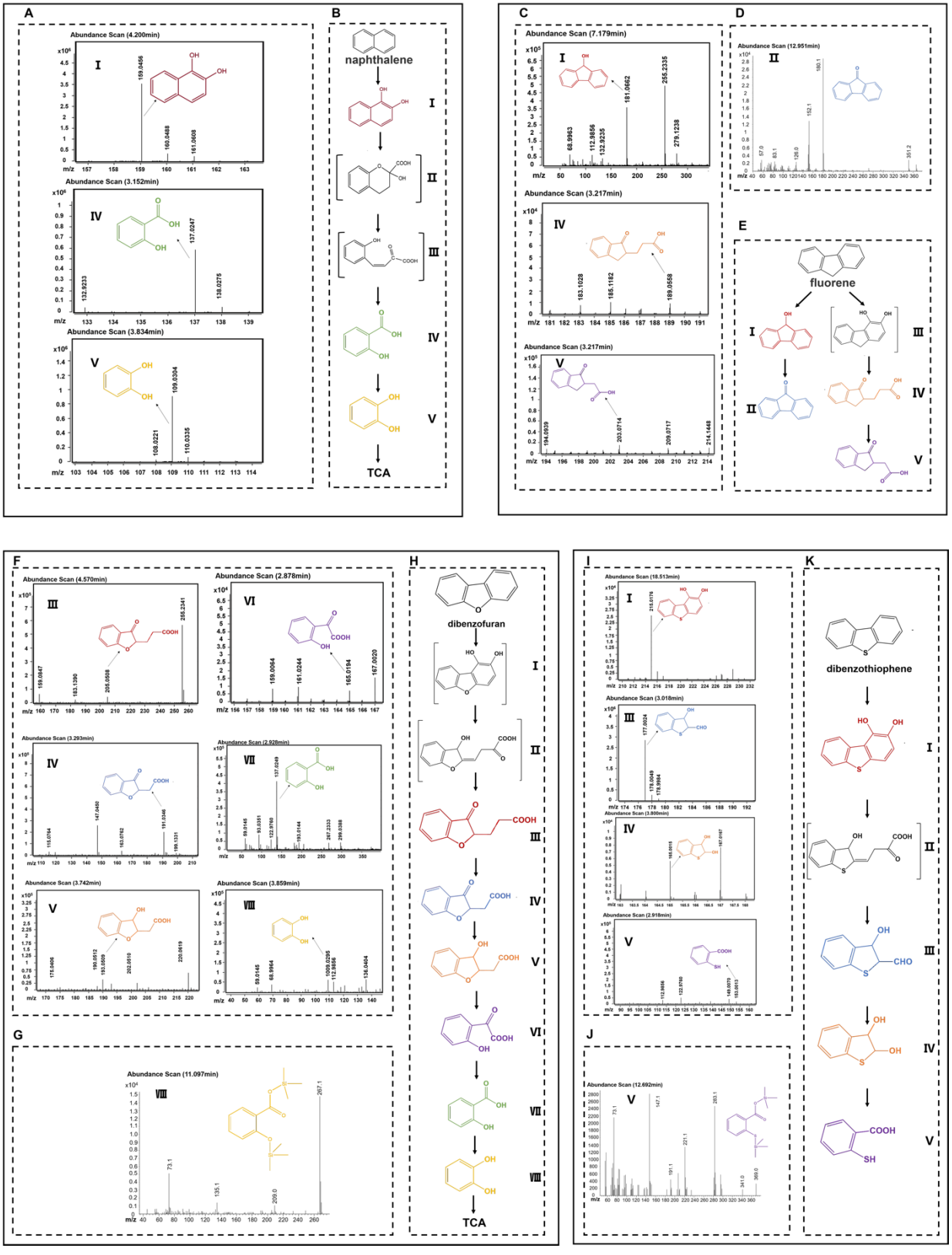
A
Abundance Scan (4.200min)
Abundance Scan (3.152min)
Abundance Scan (3.834min)
B
naphthalene
TCA
C
Abundance Scan (7.179min)
Abundance Scan (3.217min)
Abundance Scan (3.217min)
D
Abundance Scan (12.951min)
E
fluorene
F
Abundance Scan (4.570min)
Abundance Scan (2.878min)
Abundance Scan (3.293min)
Abundance Scan (2.928min)
Abundance Scan (3.742min)
Abundance Scan (3.859min)
G
Abundance Scan (11.097min)
H
dibenzofuran
TCA
I
Abundance Scan (18.513min)
Abundance Scan (3.018min)
Abundance Scan (3.800min)
Abundance Scan (2.918min)
J
Abundance Scan (12.692min)
K
dibenzothiophene

Fig. 5

A

Control	Case	Up-regulated Genes	Down-regulated Genes	Total DEGs
CK	DBF	487	383	870

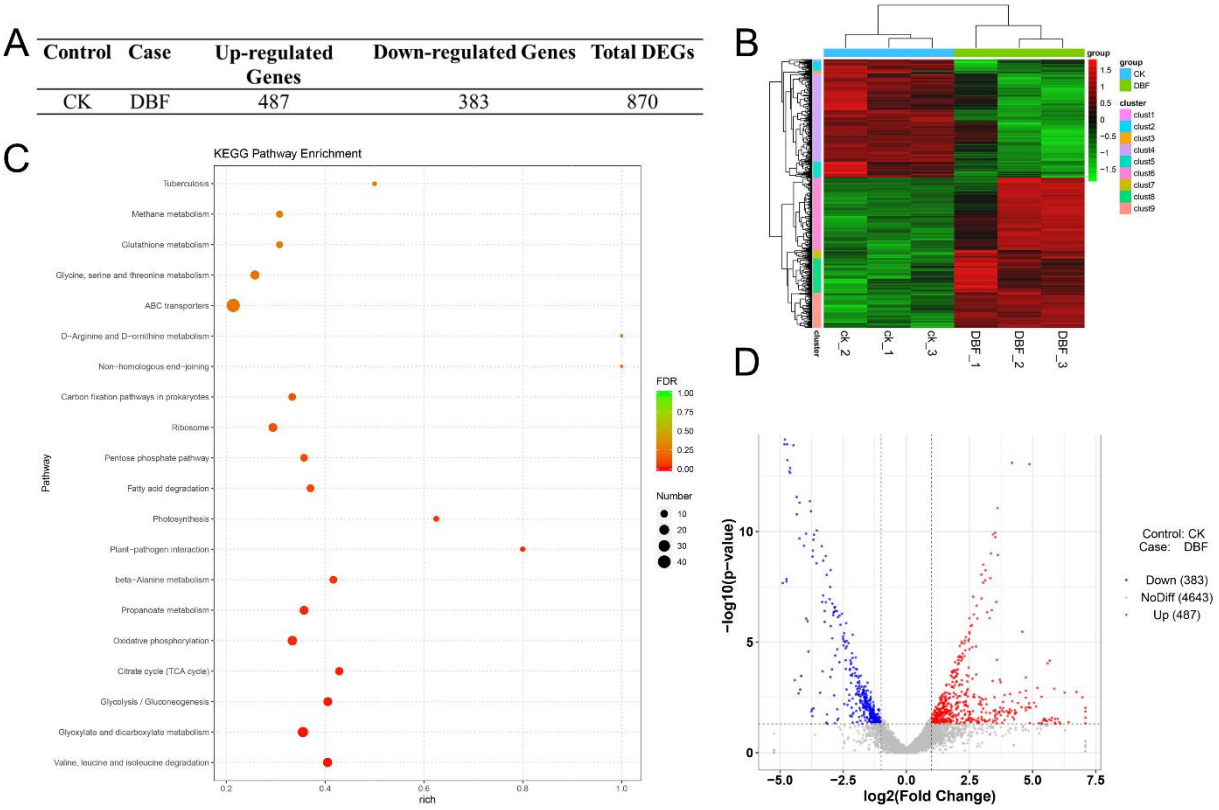

Fig. 6

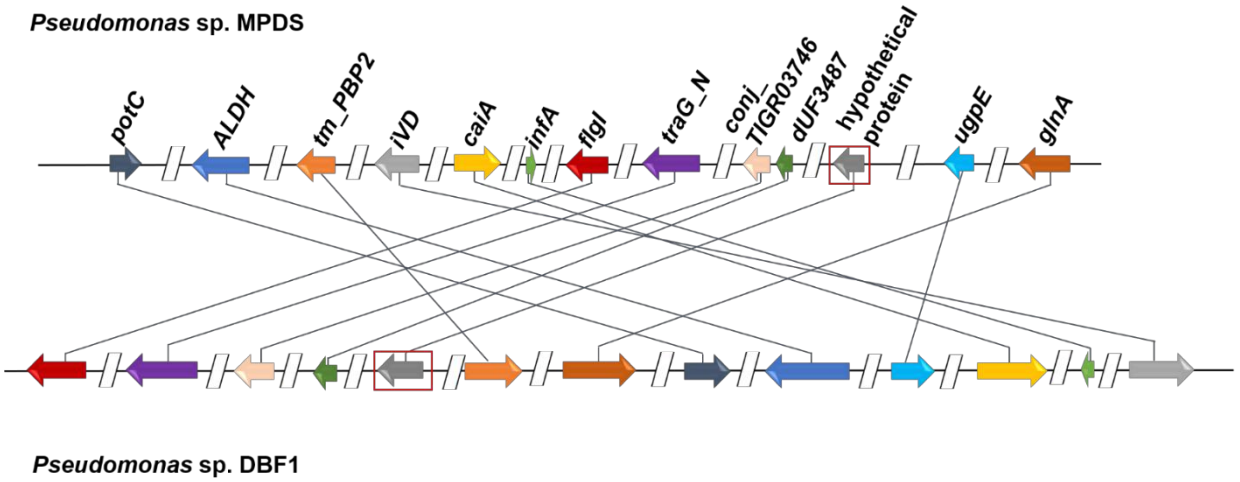
Pseudomonas sp. MPDS
potC
ALDH
tm_PBP2
iVD
caiA
infA
flgI
traG_N
conj_
TIGR03746
dUF3487
hypothetical
protein
ugpE
glnA
Pseudomonas sp. DBF1

Fig. 7

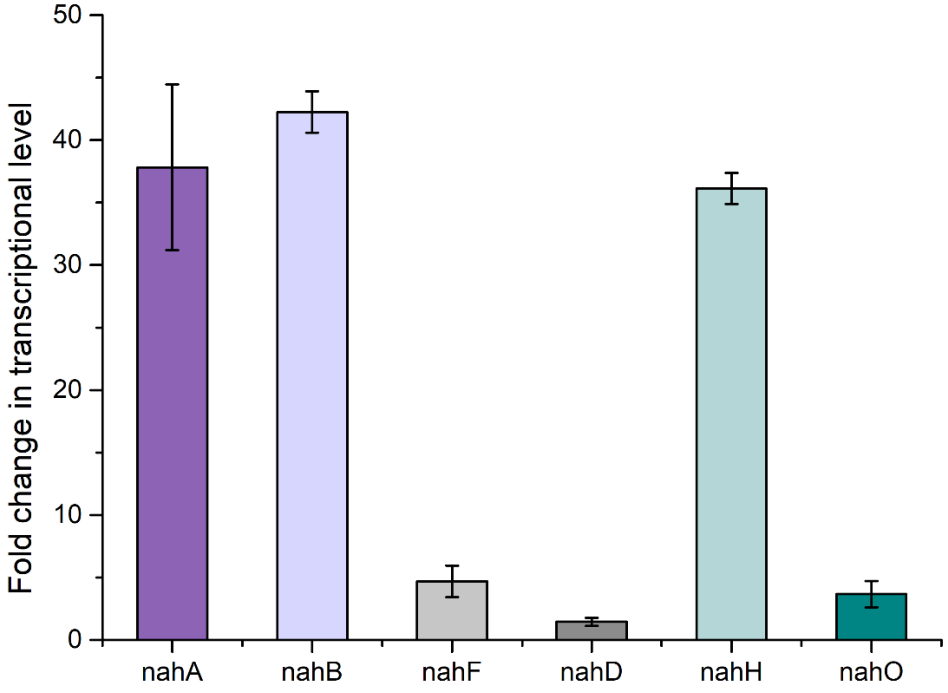
Fold change in transcriptional level
50
40
30
20
10
0
nahA
nahB
nahF
nahD
nahH
nahO

Table 1. Antibiotic resistance of strain MPDS

Antibiotic	Average diameter of bacteriostatic circle(cm)	Antibiotic resistance
Amikacin	2.680	S
Tetracycline	3.025	S
Kanamycin	2.375	S
Gentamicin	1.800	S
Piperacillin	3.450	S
Fosfomycin	3.625	S
Streptomycin	1.325	I
Rifampicin	1.925	I
Ciprofloxacin	1.725	I
Lincomycin	0.750	R
Amoxicillin	0.700	R
Norfloxacin	0.950	R
Chloramphenicol	0.700	R
Cefazolin	0.700	R
Nitrofurantoin	0.700	R
Penicillin	0.700	R
Ampicillin	0.700	R
Vancomycin	0.700	R
Erythromycin	0.700	R
Clindamycin	0.700	R

R: resistance, I: intermediary, S: sensitivity.